

SpaCE-10: A Comprehensive Benchmark for Multimodal Large Language Models in Compositional Spatial Intelligence

Ziyang Gong^{1,2*}, Wenhao Li^{3,2*}, Oliver Ma², Songyuan Li⁴, Jiayi Ji^{3,5},
Xue Yang¹, Gen Luo², Junchi Yan¹, Rongrong Ji³
¹ Shanghai Jiao Tong University ² Shanghai AI Laboratory
³ Xiamen University ⁴ Sun Yat-sen University ⁵ National University of Singapore

*Equal contribution



Project Page



Evaluation



Dataset

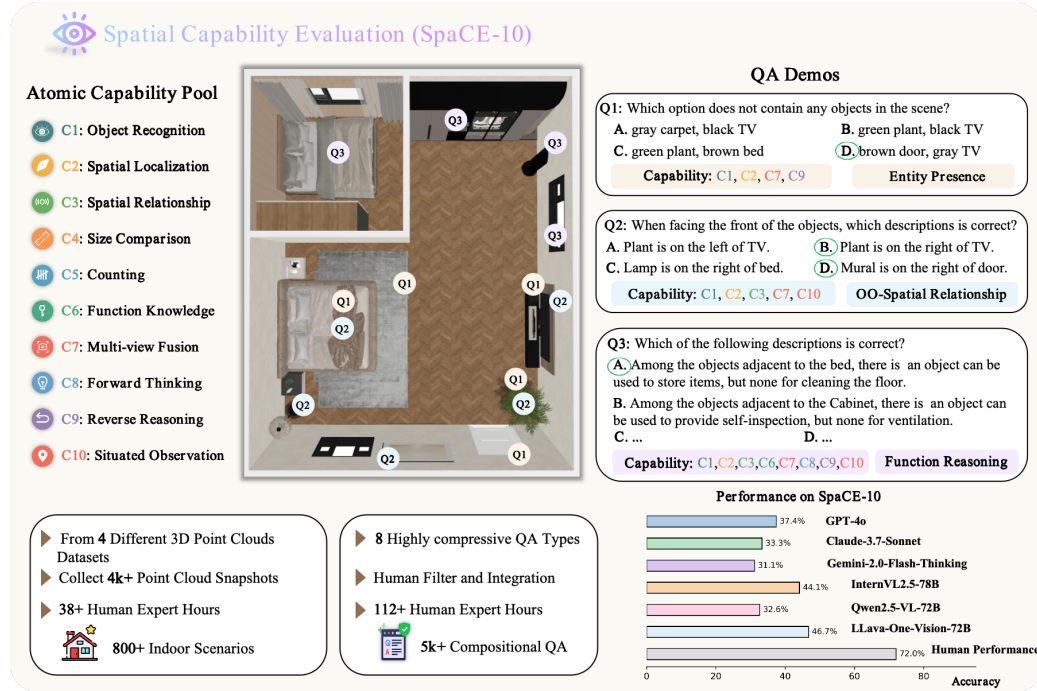


Figure 1: **Overview of SpaCE-10 benchmark.** SpaCE-10 takes over 150 human expert hours to collect 5k+ QA pairs in 811 indoor scenes, which can evaluate MLLMs from 10 atomic capabilities to 8 compositional capabilities. Through extensive evaluations, SpaCE-10 indicates that even the most advanced MLLM still lags far behind humans by large margins.

Abstract

Multimodal Large Language Models (MLLMs) have achieved remarkable progress in various multimodal tasks. To pursue higher intelligence in space, MLLMs require integrating multiple atomic spatial capabilities to handle complex and dynamic tasks. However, existing benchmarks struggle to comprehensively evaluate the spatial intelligence of common MLLMs from the atomic level to the compositional

level. To fill this gap, we present SpaCE-10, a comprehensive benchmark for compositional spatial evaluations. In SpaCE-10, we define 10 atomic spatial capabilities, which are combined to form 8 compositional capabilities. Based on these definitions, we propose a novel hierarchical annotation pipeline to generate high-quality and diverse question-answer (QA) pairs. With over 150+ hours of human expert effort, we obtain over 5k QA pairs for 811 real indoor scenes in SpaCE-10, which covers various evaluation settings like point cloud input and multi-choice QA. We conduct an extensive evaluation of common MLLMs on SpaCE-10 and find that even the most advanced MLLM still lags behind humans by large margins. Through our careful study, we also draw several significant findings that benefit the MLLM community. For example, we reveal that the shortcoming of counting capability greatly limits the compositional spatial capabilities of existing MLLMs. The evaluation code and benchmark datasets are available at [here](#).

1 Introduction

Recent years have witnessed the rapid development of multimodal large language models (MLLMs) [2, 50, 1, 12, 5, 26, 25], which continually narrows the gap between machines and humans in various multimodal tasks [37, 44, 22, 9, 27]. The significant progress has motivated researchers to pursue higher machine intelligence in the real world [21, 19, 45, 20, 56, 18, 29, 39, 15]. As shown in Fig. 1, when situated in a real scene, the machine needs to perceive the surrounding environment, collect key content, analyze visual cues, and perform interactions. This places a higher demand on existing MLLMs in compositional spatial intelligence, where multiple atomic spatial capabilities should be integrated together in task solving. Therefore, a question is naturally raised: *Can existing MLLMs master atomic space capabilities and seamlessly combine them?*

Nevertheless, this question still remains unanswerable via existing evaluation benchmarks [63, 41, 4, 43, 58, 31]. As shown in Tab. 1, early benchmarks [4, 43, 58, 63, 8] mainly focus on the assessment of atomic capabilities like object recognition and spatial localization, while compositional ones still remain to be defined and evaluated. Recently, VSI-Bench [61] aims to evaluate the visual-spatial intelligence of MLLMs through more compositional questions, but still fails to reflect the role of different atomic capabilities in compositional reasoning. More importantly, existing spatial benchmarks struggle to satisfy the evaluation needs of existing MLLMs in terms of scenes, modalities, and question types, *etc.* As shown in Tab. 1, the number of scenarios in existing benchmarks is usually less than 400, which makes it difficult to cover various practical situations.

To fill these gaps, we present SpaCE-10, a comprehensive benchmark for compositional **Spatial Capability Evaluation** of MLLMs. In SpaCE-10, we first define 10 atomic spatial capabilities that common MLLMs should master in the real world, *e.g.*, object recognition and spatial localization. Based on these atomic capabilities, we construct a pool of compositional capabilities, each of which requires combining multiple atomic ones. As shown in Fig. 1, one question-answer pair often consists of more than 3 atomic capabilities. Therefore, SpaCE-10 can not only assess the compositional spatial capabilities of MLLMs, but can also reflect the impact of different atomic capabilities in compositional reasoning.

Based on this design principle, we propose an innovative hierarchical annotation pipeline in SpaCE-10. Specifically, we collect over 800 real indoor scanned scenes from four public datasets. For each scene, we present an automated pipeline to generate structured data that can describe different types of information in the scene, *e.g.*, appearance and relationship. Based on this information, a multi-stage semi-automated pipeline is adopted to generate basic QA pairs, conduct quality verification, and perform the capability integration. Our SpaCE-10 consists of more than 5,000 high-quality QA pairs, covering various settings of existing MLLMs, *e.g.*, point cloud input and multi-choice question types. As shown in Tab. 1, SpaCE-10 demonstrates greater diversity than previous benchmarks in data distribution, annotation process, and evaluation settings, showing promising all-around evaluation ability for compositional spatial intelligence.

We conduct extensive and systematic evaluations of mainstream MLLMs on SpaCE-10, including 3 close-source MLLMs and more than 20 open-source MLLMs ranging from 2B to 78B. Experimental results show that even the most advanced MLLMs are still far behind humans in compositional spatial intelligence, *i.e.*, 37.4% of GPT4o vs. 72.0% of human. Meanwhile, 2D MLLMs demonstrate much

Table 1: **Comparison of SpaCE-10 with existing spatial benchmarks.** Our SpaCE-10 contains the most diverse scenarios and QA types, covering various evaluation settings of existing MLLMs.

Dataset	Scenario Source	Scene	Q&A	Metric	2D & 3D	Multi-Choice	Multi-Capability
3DQA [68]	SCN [13]	-	902	Sim.	×	×	×
ScanQA [4]	SCN [13]	167	10k	Sim.	✓	×	×
FE-3DGQA [68]	SCN [13]	100	3.9k	Sim.	×	×	×
SQA3D [43]	SCN [13]	132	6.9k	Sim.	✓	×	×
CLEVER3D [58]	SCN [13]	133	10k	Sim.	×	×	×
3D-LLM [19]	OBJ,SCN [13],HM3D [47]	-	30k	Sim.	×	×	×
M3DBench [28]	SCN [13]	-	1.5k	Sim.+LLM	×	×	×
MSQA [31]	SCN [13],3RS [54],ARK [7]	381	3.5k	LLM	×	×	×
VSI [61]	SCN [13],3RS [54],SCN++ [64]	288	5.0k	Acc.	×	×	✓
SpaCE-10 (Ours)	SCN [13],3RS [54],ARK [7],SCN++ [64]	811	6k	Acc.	✓	✓	✓

stronger capabilities than 3D MLLMs on SpaCE-10, showing great potential for image-based spatial reasoning. Besides, existing MLLMs greatly fall short in multiple-choice QAs, suggesting their inferior complex reasoning abilities. Our further study also reveals that the shortcoming of counting capability greatly limits the compositional spatial capabilities of existing MLLMs. These findings provide valuable directions for the community to develop more capable MLLMs. Overall, our main contributions are summarized as follows:

- We present SpaCE-10, a comprehensive benchmark for compositional spatial intelligence. SpaCE-10 is the most diverse benchmark that can assess the capabilities of MLLMs from the atomic level to the compositional level. It also covers various evaluation settings, including 3D inputs and multi-choice questions.
- We propose an innovative hierarchical annotation pipeline in SpaCE-10, which first produces structured descriptions of scenes via an automated pipeline and then generates compositional QA pairs through a multi-stage semi-automated pipeline. The hierarchical pipeline ensures the quality, diversity, and controllability of the generated QA pairs.
- We conduct extensive evaluations for nearly 30 open- and close-source MLLMs on SpaCE-10. Through our in-depth analysis, we draw several significant findings that will benefit the deployment of future MLLMs in the community.

2 Related Work

2.1 Multimodal Large Language Models

Advancements in large language models (LLMs) have led to the development of multimodal large language models (MLLMs) like GPT [2], Claude [1], Gemini [50, 51], and open-source models such as BLIP [26, 25, 14], LLaVA [34, 33, 24], Qwen [5, 59, 6, 60], and InternVL [12, 11, 10, 70, 40]. However, studies [53, 41, 61] reveal that MLLMs still struggle with visual spatial intelligence, particularly in understanding object relationships, positions, and maintaining consistency across viewpoints. Recent efforts [56, 16, 21, 69, 45] to integrate 3D point clouds data with 2D images have improved spatial reasoning but still face challenges in aligning geometric and semantic information, limiting their real-world applicability.

2.2 Multimodal QA Benchmarks

With the expanding capabilities of MLLMs, an increasing number of studies have focused on systematically evaluating their performance across diverse tasks, including caption generation [9, 3, 65], visual question answering (VQA) [22, 44, 17, 71, 36, 37, 48, 38], and code generation [27]. Among these tasks, VQA has emerged as one of the most widely adopted formats due to its alignment with human interaction paradigms. Despite strong performance on general VQA tasks, assessing MLLMs’ spatial intelligence remains a major challenge. Existing benchmarks in this area fall into two main categories. The first [55, 57] focuses on 2D abstract reasoning, using logic puzzles or geometric patterns to test panel spatial reasoning. The second [41, 4, 43, 32, 61, 23, 62, 42, 67, 49]

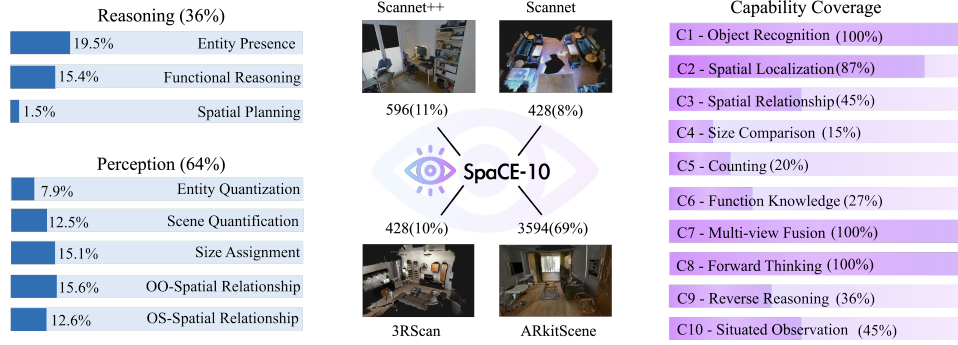


Figure 2: **Statistics of SpaCE-10.** (Left) Distribution of 8 compositional question types in SpaCE-10. (Middle) Proportion of questions across different scenarios. (Right) The 10 atomic capabilities evaluated in SpaCE-10 and their coverage across all questions.

explores realistic scene understanding, using natural images or 3D point clouds data. Our SpaCE-10 begins from the capability and evaluates MLLMs’ compositional spatial intelligence.

3 SpaCE-10

3.1 Data Collection

SpaCE-10 comprises several 3D indoor-scene scan datasets, including ScanNet++[64], ScanNet[13], 3RScan [54], and ARKitScene [7]. For scene selection, we use the ScanQA [4] test set for sampling scenes from ScanNet, and select scenes from the validation and test sets of the other scan datasets. To support both 2D and 3D data inputs, we collect the official 2D frames corresponding to the 3D scans from each dataset. The final dataset consists of over 800 real indoor scenes, including a wide variety of indoor environments such as living rooms, classrooms, bathrooms, kitchens, and more. The dataset also includes more than 5,000 high-quality question-answer pairs. The number of QA pairs in each scan dataset is detailed in Figure 2 (Middle).

3.2 Hierarchical Annotation Pipeline

Overview. As shown in Fig 3 (a), our annotation pipeline consists of 5 stages from data preparation to high-quality QA generation. In stage-1, we employ human experts to manually collect snapshots of 3D point cloud scans from 4 to 6 different views, which costs over **38 hours** of human expertise to check the quality of snapshots. In stage-2, we combine the collected snapshots and video frames to generate the structural data of describes different information in the scene. Then, we use this data to generate over 10k basic QAs covering atomic capabilities. In stage-4, human experts will manually filter the low-quality QA pairs, costing over **112 expert hours** and resulting in over 8k+ QA pairs. Finally, we design a cross-capability integration strategy to mix QAs of different atomic capabilities into a single one, yielding the final QA pairs covering 8 compositional spatial capabilities.

Structural Data Generation.

As shown in Fig. 3 (b), this pipeline follows a progressive design with 6 steps: (1) In step-1, we select 10 keyframes from the video of each scenario by combining the CLIP vision encoder [46] and the k-means algorithm. (2) In step-2, we leverage GPT-4o to generate a 2D caption for each scene, which covers information of appearance, size, and spatial relationships. (3) In step-3, we reuse GPT-4o as an inspector to refine the 2D captions by removing incorrect and redundant information. (4) In step-4, our manually collected 3D snapshots will be combined with keyframes for 3D caption generation. These high-quality snapshots contain rich global information about the whole scenes, which can provide considerable scene-level spatial information. (5) In step-5, we leverage an inspector again to further check and refine the spatial descriptions. (6) Finally, we employ a rule-based extractor to obtain structural data for the following QA generation.

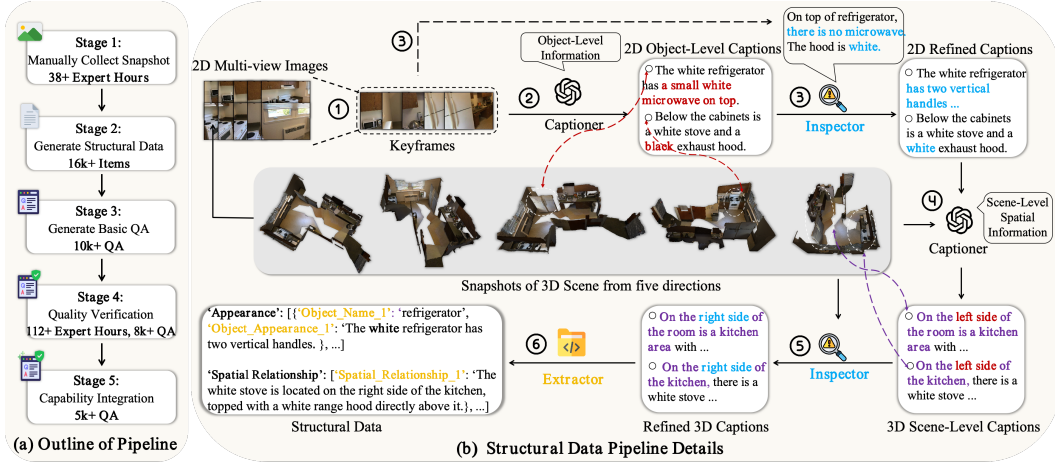


Figure 3: **Illustration of our hierarchical annotation pipeline.** We generate structural data to construct over 10k QA pairs, and performs capability integration to obtain over 5k QA pairs with 10 compositional capabilities. This process takes over 150 expert hours for data collection and filtering.

Basic QA Generation. As we mentioned earlier, the questions in SpaCE-10 are composed of multiple atomic capabilities. However, such highly integrated questions are difficult for current MLLMs to generate directly. Therefore, we propose to first generate a basic version of QA, namely basic QA, and then enhance its embedded capabilities. Next, we will briefly introduce the QA types in SpaCE-10. As shown in Fig. 2, SpaCE-10 consists of 8 QA types, including Entity Quantification (EQ), Region Quantification (RQ), Size Assessment (SA), Object-Object Spatial Relationship (OO), Object-Scene Spatial Relationship (OS), Functional Reasoning (FR), and Spatial Planning (SP). All QA pairs are split into Reasoning and Perception. For the Fig. 2 (Left), perception includes 5 sub-types, accounting for $\sim 70\%$ of the questions, and reasoning includes 3 sub-types, comprising $\sim 30\%$ of the questions.

During the basic QA generation, we adopt 3 approaches: template-based, MLLM-based, and human-based generation. For EQ, we first extract the number of each object from the scan datasets’ semantic labels, and then leverage GPT-4o to generate QA. For the SP, we employed human experts to manually design 80 QA pairs focused on tidying a room. Each question presents a complete task flow, including the navigation path, goal, goal characteristics, and actions to be performed, with potential errors in any step. Based on the prompt, the model must select either a fully correct task flow or one containing incorrect steps. For the rest of the QA types, we generate based on structural data by GPT-4o. Moreover, 5 types of QA will be applied with a cross-capability mixture, and we will introduce them next.

Cross-Capability Integration Strategy. After generating the basic QA, we proceed to enhance the capabilities of the five types of questions in the basic QA. Before introducing the enhancement, we briefly describe the atomic capabilities. SpaCE-10 establishes an atomic capability pool, including C1 to C10: Object Recognition, Spatial Localization, Spatial Relationship, Size Comparison, Counting, Function Knowledge, Multi-view Fusion, Forward Thinking, Reverse Reasoning, and Situated Observation. As shown in Fig. 2 (Right), in the capability pool, the most frequently utilized capabilities are C1, C2, C7, and C8, forming the spatial perception foundation of MLLMs. Higher-level abilities, such as C3, C9, and C10, are tested in approximately 50% of the questions, enhancing the model’s spatial reasoning ability. More details of capabilities are provided in the supplementary material.

Based on these atomic capabilities, we apply three strategies to integrate cross-capabilities into five types of QA: (1) For SA, OO, and OS, we integrate an additional C7. In the original basic QA, each option involves only a single object from the same scene. For OO and OS, we enhance them from single-object examinations to multiple objects from the same scene in each option, converting a single view to multiple-view fusion. Additionally, for OS, we slightly adjust the strategy by combining multiple spatial relationships into a single question, e.g., left, right, farthest, nearest, and so on. This integration forces the model to fully comprehend the entire scene, enabling a more holistic spatial perception. (2) For EP, we add C7 and C9, expanding the question to involve multiple objects. We then reverse the question type from “which object exists” to “which object does not exist,” integrating

reverse reasoning capabilities. (3) For FR, we add C7, C9, and C10. The basic question asks which option correctly describes the function of an object near a given central object. The options are structured as <Object1>, <Function>.... In the integrated version, the question is revised to: “Which of the following is correct?” Each option now involves a different central object, with the structure: “Among the objects adjacent to <Central Object1>, one can be used for <Function>, while none of the others can.” This change prevents potential leakage of prior knowledge, such as object names, and places greater emphasis on the model’s understanding of functional roles. Similar to the previous strategy, the task scope is expanded to cover the entire scene.

3.3 Quality Verification

For the quality verification process, we rely on manual screening by human experts. We set up a validation framework based on Gradio and employed two human experts to perform the evaluation. In this process, the evaluation criteria include checking for incorrect options, invalid answers, missing data, or questions involving objects not present in the snapshots. This quality control process takes over 112 hours to check and filter low-quality QA pairs. By employing human validation, we ensure that only high-quality and contextually accurate questions are retained for the final benchmark. Related visualizations are attached in the supplementary material.

4 Experiments

4.1 Setup

In our experiments, we test extensive close-source and open-source MLLMs on SpaCE-10, including 3D MLLMs leo [21], MLLMs for 3D GPT4Scene [45], GPT-4o [2], Gemini-2.0 [50], Claude-3.7-sonnet [1], InternVL2.5 [10], Qwen2.5-VL [6], and so on. During the evaluation, except for Leo, which is evaluated by their own framework, other MLLMs are evaluated by the LMMs-Eval [66], and open-source MLLMs are tested on Tesla A100 GPUs. For the response and answer alignment, we follow the prompt of mmbench [37] and use GPT-4o-2024-11-20 for the judgment. Notably, we removed the random assignment in LMMs-Eval, so the model’s performance is likely to be lower than the random baseline (25% for single choice, 10% for double choice).

4.2 Overall Results

Human vs. MLLMs. We first test human performance on SpaCE-10, taking the average score of two humans to obtain the ‘Human’ score in Tab. 2. The results indicate that although human performance does not meet expectations when facing with more complex numerical and reasoning tasks, the total score of 81.5% is still significantly higher than all existing MLLMs. In comparison, the best open-source MLLM only achieves an average score of 52.8%, and the best close-source models only achieve a score of 49.0%. These results demonstrate that the compositional spatial intelligence of MLLMs is far below the human level.

3D MLLMs vs. 2D MLLMs. In Tab. 2, we evaluate LEO and GPT4Scene as representatives of 3D-related MLLMs. Notably, input to the LEO model requires point clouds of the objects relevant to the questions. To ensure a fair comparison, we adjust the input for LEO by randomly sampling 1024 points from the entire scene’s point clouds. The results show that LEO scored 11.1% overall in SpaCE-10, which is significantly lower than GPT4Scene (31.9%). Compared with InternVL2.5-1B, the performance of LEO, which has 7B parameters, is also substantially lower. We argue that one of the limitations of current 3D MLLMs is that they are designed to focus on specific objects and have difficulty processing the entire scene’s point clouds as input. Additionally, they likely sacrifice multimodal conversational abilities for understanding scans. These results also indicate that 2D MLLMs have greater potential in visual spatial intelligence comprehension than 3D MLLMs.

Open-Source vs. Close-Source. In close-source MLLMs experiments, GPT-4o-2024-11-20 [2] achieves the best overall performance, ranking 4th with a score of 49.0%. It excels in perception tasks, such as in SA with 56.2%, OO with 58.3%, and OS with 56.2%, indicating strong accuracy in recognizing size and position. Additionally, GPT-4o [2] achieves the highest score in EQ among all tested models, with a score of 58.3%. However, it struggles with SP, where it scores the lowest among all tasks, suggesting a limitation in scene-level planning ability. Gemini-2.0-Flash-Thinking-exp [50] and Claude-3.7-Sonnet-20250219 [1] achieve overall scores of 42.2% and 46.2%, respectively.

Table 2: **Single-choice performance ranking of existing MLLMs on SpaCE-10 benchmark.** The annotations like $\times 0.5$ represent the weights to the Overall Performance.

Models	Rank	Perception					Reasoning			Overall
		EQ $\times 0.09$	SQ $\times 0.15$	SA $\times 0.13$	OO $\times 0.15$	OS $\times 0.11$	EP $\times 0.20$	FR $\times 0.15$	SP $\times 0.02$	
Human	1	63.6	78.9	80.2	82.3	88.1	81.8	90.6	78.6	81.5
3D MLLMs										
LEO-7B [21]	26	15.8	0.0	16.7	16.5	25.2	5.5	5.7	13.3	11.1
GPT4Scene-Qwen2-VL-7B [45]	16	30.9	37.7	38.0	38.9	41.6	29.5	28.0	32.5	31.9
Close Source 2D MLLMs										
GPT-4o-2024-11-20 [2]	4	58.3	32.8	56.2	58.3	56.2	41.6	52.2	23.7	49.0
Gemini-2.0-Flash-Thinking-Exp [50]	10	34.3	25.6	53.1	42.6	53.8	42.2	46.7	31.2	42.2
Claude-3.7-Sonnet-20250219 [1]	7	46.0	44.3	49.1	46.0	49.1	44.3	49.3	25.0	46.2
Open Source 2D MLLMs										
▼ Scale < 7B										
InternVL2.5-1B [10]	13	33.0	54.1	18.8	43.6	29.9	30.9	41.0	23.7	36.2
InternVL2.5-2B [10]	18	32.2	26.8	27.0	36.6	28.8	34.0	48.2	36.2	33.8
Qwen2.5-VL-3B-Instruct [59]	15	31.7	23.3	47.1	51.7	31.6	25.5	37.0	21.2	34.8
SpaceOm \diamond	20	21.8	24.5	47.3	49.7	32.7	21.9	36.7	25.0	33.2
SpaceQwen \diamond	14	31.2	26.1	41.2	52.3	35.2	28.4	36.4	22.5	35.4
SpaceThinker-Qwen2.5VL-3B \diamond	17	32.7	22.4	46.7	50.5	33.4	22.4	36.9	24.2	34.1
VILA1.5-3B [30]	24	25.0	9.1	31.7	34.6	31.6	35.3	12.9	33.7	26.1
InternVL2.5-4B [10]	11	34.3	23.4	50.2	50.8	16.2	38.3	56.0	33.7	39.3
▼ Scale < 13B										
Qwen2.5-VL-7B-Instruct [59]	19	32.7	36.9	36.9	35.3	32.3	27.6	34.2	27.5	33.3
LLaVA-v1.5-7B [35]	22	31.2	31.3	30.5	35.7	22.9	10.7	57.4	32.5	30.7
LLaVA-OneVision-7B [24]	8	37.4	33.8	46.4	57.3	34.5	43.3	61.6	21.2	45.2
Cambrian-8B [52]	23	22.6	18.6	34.8	32.6	32.3	25.1	41.4	23.7	29.5
VILA1.5-8B [30]	25	25.7	8.21	27.5	32.7	17.2	12.4	26.7	23.7	20.9
InternVL2.5-8B [10]	9	33.2	36.0	50.0	55.0	33.6	41.1	59.1	32.5	44.6
▼ Scale < 72B										
InternVL2.5-26B [10]	6	34.3	29.3	62.6	55.4	33.0	50.2	61.8	33.7	47.5
Qwen2.5-VL-32B-Instruct [59]	21	19.9	26.5	48.9	36.8	32.3	31.1	30.1	32.5	32.6
InternVL2.5-38B [10]	5	38.1	36.1	64.4	54.3	36.8	45.6	63.0	37.5	48.7
▼ Scale > 72B										
LLaVA-OneVision-72B [24]	2	44.1	38.3	67.9	64.5	40.3	46.7	67.3	36.2	52.8
Qwen2.5-VL-72B-Instruct [59]	12	32.4	34.9	55.7	40.9	32.1	36.5	38.0	33.7	37.9
InternVL2.5-78B [10]	3	27.8	45.0	62.4	64.4	40.3	36.6	67.3	40.0	49.7

\diamond Models proposed by RemyxAI (SpaceVLMs series, <https://huggingface.co/remyxai/SpaceQwen2.5-VL-3B-Instruct>).

Compared to these models, Claude-3.7-Sonnet shows a more balanced performance across tasks. In open-source MLLMs, among models with a scale of over 72B, LLaVA-OneVision-72B delivers outstanding performance, ranking first overall with a score of 52.8%. It outperforms other models in nearly all tasks, solidifying its top position. Furthermore, InternVL2.5-78B achieves the second-highest score of 49.7%, showing the increasing competitive edge of open-source models in spatial reasoning. These results suggest that the gap between open-source and close-source models has significantly narrowed, and open-source MLLMs even outperform close-source models, especially in compositional spatial intelligence.

Single-Choice vs. Multiple-Choice. The results in Tab. 3 show that MLLMs perform significantly worse on multiple-choice tasks compared to single-choice tasks. Smaller models like InternVL2.5-1B and 2B score over 30.0% on single-choice tasks, while in multiple-choice tasks, their scores often fall below 5%, which is even worse than random selection. As the model size increases to 78B, MLLMs show greater robustness for different QA types. These results lead to an interesting preliminary

Table 3: **Performance of MLLMs on single-choice and multiple-choice QA pairs.** Results show that existing models, especially smaller ones, tend to overfit to single-choice questions.

Models	Single-choice (3091)					Multiple-choice (970)					Overall ↑		Score ↑
	SA	OO	OS	EP	FR	SA	OO	OS	EP	FR	Single	Multiple	multiple / single
InternVL2.5 Series													
InternVL2.5-1B [10]	18.8	43.6	29.9	30.9	41.0	4.4	3.9	4.7	0.5	11.4	32.8	3.0	0.09
InternVL2.5-2B [10]	27.0	36.6	28.8	34.0	48.0	4.7	2.0	1.3	1.5	3.5	34.9	4.1	0.12
InternVL2.5-8B [10]	50.0	55.0	33.6	41.1	59.1	8.4	14.8	8.7	12.9	1.5	47.8	10.6	0.22
InternVL2.5-38B [10]	64.4	54.3	36.8	45.6	63.0	47.8	37.9	7.3	21.3	46.8	52.8	32.2	0.61
InternVL2.5-78B [10]	62.4	64.4	40.3	36.6	67.3	38.4	33.5	12.1	12.9	45.8	54.2	28.5	0.53
Qwen Series													
Qwen2.5-VL-3B-Instruct [6]	47.1	51.7	31.6	25.5	37.0	21.7	24.1	8.0	15.3	20.7	38.6	17.9	0.46
Qwen2.5-VL-7B-Instruct [6]	36.9	35.3	32.3	27.6	34.2	20.2	11.8	14.7	13.4	10.4	33.3	14.1	0.42
Qwen2.5-VL-32B-Instruct [6]	48.9	36.8	32.3	31.1	30.1	25.6	6.9	8.0	10.4	12.9	35.8	12.8	0.36
Qwen2.5-VL-72B-Instruct [6]	55.7	40.9	32.1	36.5	38.0	17.2	13.3	13.0	15.7	15.9	40.6	15.0	0.37
Others													
Cambrian-8B [52]	34.8	32.6	32.3	25.1	41.4	5.9	12.8	5.9	0.5	20.6	33.2	9.1	0.27
VILA1.5-8B [30]	27.5	32.7	17.2	12.4	26.7	0.0	0.5	1.5	2.0	26.9	23.3	6.2	0.27
LLaVA-OneVision-72B [24]	67.9	64.5	40.3	46.7	67.3	38.9	32.0	13.3	34.7	35.8	57.3	30.9	0.54

conclusion: smaller models may overfit to the single-choice task format, while larger models seem to have learned more fundamental compositional spatial intelligence. However, the Qwen series exhibits an almost opposite trend, with high scores in the smaller models, reaching 0.46. As the parameters increase, the scores slightly decrease, but overall, the performance remains normal.

Table 4: **Accuracy comparison on basic and compositional QA pairs.** The results reveal the relationship between the performance and integration of capacities.

Task	Integrated	Capability	InternVL2.5-1B	8B	Qwen2.5-VL-3B	7B	Overall-C(%)
SA	×	C1,C2,C4,C8	37.8	66.4	60.0	64.8	57.3
	✓	+C7	18.8 (↓ 19.0)	50.0 (↓ 16.4)	47.1 (↓ 12.9)	36.9 (↓ 27.9)	38.2 (↓ 19.1)
OO	×	C1,C2,C3,C8,C9,C10	52.0	66.4	56.4	41.2	54.0
	✓	+C7	43.6 (↓ 8.4)	55.0 (↓ 11.4)	51.7 (↓ 4.7)	35.3 (↓ 5.9)	46.4 (↓ 7.6)
OS	×	C1,C2,C3,C9,C10	44.2	54.8	50.8	54.3	51.0
	✓	+C7	29.9 (↓ 21.6)	33.6 (↓ 21.2)	31.6 (↓ 19.2)	32.3 (↓ 22.0)	30.0 (↓ 21.0)
EP	×	C1,C2,C8	66.6	75.8	63.4	65.3	67.8
	✓	+C7,C9	30.9 (↓ 35.7)	41.1 (↓ 34.7)	25.5 (↓ 37.9)	27.6 (↓ 37.7)	31.3 (↓ 36.5)
FR	×	C1,C2,C3,C6,C8	70.9	89.7	85.6	85.7	83.0
	✓	+C7,C9,C10	41.0 (↓ 29.9)	59.1 (↓ 30.6)	37.0 (↓ 48.6)	34.2 (↓ 51.5)	42.8 (↓ 42.9)

4.3 Capability Analysis

Atomic Capability vs. Compositional Capabilities. Firstly, the Tab. 4 shows that on the 5 types of questions with more compositional abilities, the performance of the four models all drops significantly. For the 3 questions with integrating C7 capability, the models’ accuracy in SA, OO, and OS tasks decreases by 19.1%, 7.6%, and 21.0%, respectively. Despite the drop, the accuracy of SA and OO still remains at a decent level. Secondly, in the EP task with both C7 and C9 abilities integrated, the models’ overall accuracy plummets from 67.8% without integration to 31.3%, a huge drop of 36.5%. Similarly, for the FR task, which with the most compositional capacities, the four models’ average score crashes from 83.0% to 42.8%, an even larger drop of 42.9%.

These results partially reveal the relationship between accuracy and capability. As more abilities are incorporated, model performance declines to varying degrees, with some decreases even exceeding 50.0%. This indicates that current models have a limited grasp of integrated spatial intelligence, thereby highlighting the necessity of SpaCE-10.

Spatial Capability Breakdown. To better understand the strengths and weaknesses of the current MLLMs across various atomic capabilities, we constructed a model accuracy and atomic capability score matrix to associate QA accuracy with capabilities. As shown in Fig. 4, from the results, we observe several findings. Overall, different models show similar trends in capabilities such as C1

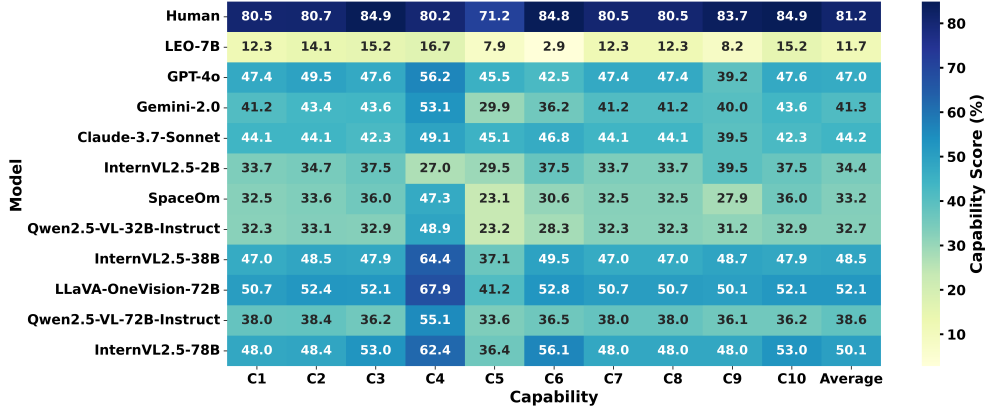


Figure 4: **Results of representative MLLMs on 10 atomic capabilities of SpaCE-10.** Each value reflects the model’s average accuracy (%) across all question types involving the respective spatial capability (C1–C10), as defined in the benchmark’s task-to-capability mapping.

(Object Recognition), C2 (Spatial Localization), C4 (Size Comparison), C6 (Functional Understanding), and C9 (Reverse Reasoning), with scores in these areas predominantly blue, indicating stable performance across models. Capabilities like C5 (Counting) show green scores, indicating weaker performance across models. Notably, the distribution of capabilities across models is relatively consistent, suggesting that while these capabilities are not fully orthogonal, models have a similar overall grasp of different abilities. Based on the macro analysis in the first step, we can now focus on the scores of each model. Similar to the accuracy trend, LLaVA-OneVision-72B demonstrates the most powerful performance, achieving the highest average scores in over seven atomic capabilities. Among all its abilities, the one with the smallest gap to human performance is C4, representing 67.9% of LLaVA-OneVision-72B with only a 12.3% difference from humans. For most models, C4 is the best mastered atomic capability, indicating that current models have relatively strong capabilities in size comparison. However, in C5, counting abilities, all models perform poorly, with the highest score reaching only 45.5% of GPT-4o, a 25.7% gap from humans. Therefore, MLLMs’ counting ability needs significant improvement.

Additionally, in terms of average scores, the best model, LLaVA-OneVision-72B, only achieved 52.1%, with a 29.1% gap from humans. The best closed-source model, GPT-4o, even has a 34.2% gap from humans. These results indicate that there is still a large room for improvement in both individual atomic spatial capabilities and integrated spatial intelligence in current MLLMs. This capability analysis provides valuable insights for guiding future enhancements of MLLMs. More experiments are attached in the supplementary materials.

5 Broader Impacts and Limitations

Although SpaCE-10 has undergone rigorous manual review, there may still be some annotation errors that slightly affect the evaluation of the model. In addition, the visual content of SpaCE-10 all comes from public datasets, which may contain some unreliable content. Besides, SpaCE-10 mainly focuses on indoor scenes, and the scene scale is relatively small, which means that the conclusions of SpaCE-10 may not be applicable to outdoor or large-scale scenes.

6 Conclusion

In this paper, we propose SpaCE-10, a comprehensive benchmark for evaluating compositional spatial intelligence in Multimodal Large Language Models (MLLMs). SpaCE-10 covers evaluations of MLLMs from 10 atomic spatial capabilities to 8 compositional capabilities. In SpaCE-10, we collect images and point clouds from 800 scenes and design a hierarchical annotation pipeline to produce over 5k high-quality question-answer pairs, covering various evaluation settings of MLLMs. To the best of our knowledge, SpaCE-10 is the most comprehensive benchmark for compositional spatial

intelligence. Through extensive evaluation, we reveal critical limitations of current MLLMs and draw several findings that are beneficial to future work in the community. We believe these studies will provide an invaluable hint for future research toward human-level machine intelligence.

A More Detailed Illustration

A.1 QA Definition

In this section, we introduce the definition of each QA type and show the QA examples in Fig. 5. Notably, each QA type is the integration of multiple capabilities, and we also show the mapping between QA and capabilities in this figure and Tab. 5. The following are definitions:

Entity Quantification (EQ): Counting the number of objects in a scene.

Scene Quantification (SQ): Counting the number of regions within a scene.

Size Assessment (SA): Comparing the size relationships between different objects.

Object-Object Spatial Relationship (OO): Understanding the relative spatial relationship between two objects.

Object-Scene Spatial Relationship (OS): Understanding the relative spatial relationship between an object and the overall scene.

Functional Reasoning (FR): Reasoning objects that match or do not match certain functions based on relative spatial relationships.

Spatial Planning (SP): Global spatial navigation and path planning.

A.2 Capability Definition

In this section, we illustrate the definition of each capability:

C1-Object Recognition: Identify what the object is.

C2-Spatial Location: Localizing an object in space.

C3-Spatial Relationship: Understanding relative spatial position relationship.

C4-Size Comparison: Comparing the size relationship of objects.

C5-Counting: Count the number of objects and scenes.

C6-Function Knowledge: Understanding the function of objects.

C7-Multi-view Fusion: Understanding spatial information from multiple views

C8-Forward Thinking: Understand the forward instructions of user instructions and execute them.

C9-Reverse Reasoning: Understand the reverse instructions of user instructions and execute them.

C10-Situated Observation: Imagine standing in a designated position in space and observing and understanding the scene.

B More Experiments

B.1 More Multiple-Choice Results

In this section, we show the single-choice and multiple-choice results of more MLLMs in Tab. 6. As we mentioned in the main paper, the multiple/single score reveals a clear trend: most small-scale models exhibit notably low scores, indicating a strong tendency to overfit to single-choice questions. This behavior reflects a reliance on shallow pattern recognition rather than a true capability for handling more compositional spatial understanding tasks. In contrast, larger models demonstrate significantly improved performance on this metric, suggesting their enhanced ability to reason over complex spatial questions.

Among the close-source MLLMs, Claude-3.7-sonnet achieves the highest score with 0.72, showing its strong ability in both single and multiple task. For the open-source MLLMs, the Qwen series stands out, with Qwen2.5-VL-32B achieving the second highest score of 0.69, showcasing strong competence in processing multi-option (double-choice) tasks that require integrative spatial reasoning. The InternVL series also performs consistently well: all larger variants (4B, 8B, 26B, 38B, 78B) surpass the 0.5 threshold, excluding only the 1B and 2B versions. These results highlight the structural advantages and training effectiveness of these models when facing combinatorial challenges. Furthermore, all close-source models (GPT-4o, Gemini, Claude) score around 0.6, demonstrating their overall strength in tasks demanding structured spatial comprehension.

Entity Presence:
Q: Which of the following options does not contain any objects in the given scene?
A. lush green plant, brown TV, blue bed, gray cabinet
B. brown lamp, blue carpet, gray TV, gray window
C. brown door, gray TV, gray window, blue cabinet
D. lush green plant, black TV, blue bed, black window
Capability: C1, C2, C7, C8, C9

Spatial Planning:
Q: Which of the following descriptions are incorrect for keeping the room clean and tidy?
A. From the entrance first move to the room center, turn left to the bed, then tidy up the quilt.
B. From the entrance first move to the room center, turn right to the bed, then tidy up the quilt.
C. From the entrance first move to the room center, turn left to the cabinet, then clean up the cabinet.
D. From the entrance first move to cabinet, turn left to the smaller room, then close the window.
Capability: C1, C2, C3, C7, C8, C9, C10

Entity Quantification:
Q: How many beds are in the given scene?
A. 1 B. 2 C. 3 D. 4
Capability: C1, C2, C5, C7, C8

Scene Quantification:
Q: The area indicated by objects with specific functions is called a functional zone (for example, a desk in the workspace, chairs and tables in the dining area). In a given scene, how many spatially different functional zones are there? A. 1 B. 2 C. 3 D. 4
Capability: C1, C5, C6, C7, C8

Size Assessment:
Q: Which descriptions is correct?
A. The door is lower than the bed.
B. The door is wider than the TV.
C. The lamp is taller than the bed.
D. The plant is lower than the bed.
Capability: C1, C2, C4, C7, C8

OO Spatial Relationship:
Q: When facing the front side of the objects, which descriptions is correct?
A. The plant is on the left of the TV.
B. The plant is on the right of the TV.
C. The lamp is on the right of the bed.
D. The mural is on the right of the door.
Capability: C1, C2, C3, C7, C8, C10

OS Spatial Relationship:
Q: When viewing from the entrance, which descriptions are correct?
A. Bed is on the center of the room.
B. TV is on the left side of the room.
C. The cabinet is the farthest object that can be seen.
D. Bed is on the right side of the room.
Capability: C1, C2, C3, C7, C8, C10

Function Reasoning:
Q: Which of the following descriptions is correct?
A. Among the objects adjacent to the bed, there is an object can be used to store items, but lacks two objects that can be used to clean the floor and to provide ventilation.
B. Among the objects adjacent to the cabinet, there is an object can be used to check appearance, but lacks two objects that can be used to provide ventilation and to rest.
C. Among the objects adjacent to the TV, there is an object can be used to check appearance, but lacks two objects that can be used to provide ventilation and to decorate the room.
D. Among the objects adjacent to the TV, there is an object can be used to decorate the room, but lacks two objects that can be used to clean the floor and to provide ventilation.
Capability: C1, C2, C3, C6, C7, C8, C9, C10

Figure 5: **Examples of all types of QA.** The blue examples represent the perception QA, and the purple ones mean the reasoning QA. The green circles are the correct answer.

Table 5: **Mapping of QA types and Spatial Capabilities.** Each type of QA is the integration of multiple capabilities.

Tasks	c1	c2	c3	c4	c5	c6	c7	c8	c9	c10
Entity Quantification (EQ)	✓	✓	-	-	✓	-	✓	✓	-	-
Scene Quantification (SQ)	✓	-	-	-	✓	✓	✓	✓	-	-
Size Assessment (SA)	✓	✓	-	✓	-	-	✓	✓	-	-
OO-Spatial Relationship (OO)	✓	✓	✓	-	-	-	✓	✓	-	✓
OS-Spatial Relationship (OS)	✓	✓	✓	-	-	-	✓	✓	-	✓
Entity Presence (EP)	✓	✓	-	-	-	-	✓	✓	✓	-
Functional Reasoning (FR)	✓	✓	✓	-	-	✓	✓	✓	✓	✓
Spatial Planning (SP)	✓	✓	✓	-	-	-	✓	✓	✓	✓

Table 6: More experiment results of multiple choices.

Models	Single-choice (3091)					Multiple-choice (970)					Overall \uparrow		Score \uparrow	
	SA	OO	OS	EP	FR	SA	OO	OS	EP	FR	Single	Multiple	multiple / single	
3D MLLMs														
GPT4Scene-Qwen2-VL-7B [45]	38.0	38.9	41.6	29.5	28.0	0.5	1.0	0.0	0.0	19.4	35.2	4.0		0.11
Close Source MLLMs														
GPT-4o-2024-11-20 [2]	56.2	58.3	56.2	41.6	52.2	16.8	36.9	41.9	12.7	35.8	52.9	28.8		0.54
Gemini-2.0-flash-thinking [50]	53.1	42.6	53.8	42.2	46.7	47.8	28.6	14.0	6.4	35.6	47.7	26.5		0.56
Claude-3.7-sonnet-20250219 [1]	49.1	46.0	53.8	44.3	49.3	35.0	33.0	13.3	25.7	41.9	48.4	31.3		0.65
Open Source MLLMs														
InternVL2.5-1B [10]	18.8	43.6	29.9	30.9	41.0	4.4	3.9	4.7	0.5	11.4	32.8	3.0		0.09
InternVL2.5-2B [10]	27.0	36.6	28.8	34.0	48.2	1.3	2.0	4.7	1.5	3.5	34.9	4.1		0.12
Qwen2.5-VL-3B-Instruct [59]	47.1	51.7	31.6	25.5	37.0	21.7	24.1	8.0	15.3	20.9	38.6	17.9		0.46
SpaceOm	47.3	49.7	32.7	21.9	36.7	19.2	24.6	9.3	0.5	20.6	37.7	14.8		0.39
SpaceQwen	41.2	52.3	35.2	28.4	36.4	17.2	26.1	10.0	1.5	35.0	38.7	17.9		0.46
SpaceThinker-Qwen2.5VL-3B	46.7	20.5	33.4	22.4	36.9	22.7	24.1	8.0	1.5	18.8	32.0	15.0		0.47
VILA1.5-3B [30]	31.7	34.6	31.6	35.3	12.9	1.0	2.5	2.0	0.0	19.4	29.2	5.0		0.17
InternVL2.5-4B [10]	50.2	50.8	16.2	38.3	56.0	22.2	24.6	4.7	0.5	10.5	42.3	12.5		0.3
Qwen2.5-VL-7B-Instruct [59]	36.9	35.3	32.3	27.6	34.2	20.2	11.8	14.7	13.4	10.4	33.3	14.1		0.42
LLaVA-v1.5-7B [35]	30.5	35.7	22.9	10.7	57.4	4.9	10.3	6.9	0.6	35.0	31.4	11.5		0.37
LLaVA-OneVision-7B [24]	46.4	57.3	34.5	43.3	61.6	21.2	22.7	10.0	5.6	37.8	48.2	19.5		0.40
Cambrian-8B [52]	34.8	32.6	32.3	25.1	41.4	5.9	12.8	5.9	0.5	20.6	33.2	9.1		0.27
VILA1.5-8B [30]	27.5	32.7	17.2	12.4	26.7	0.0	0.5	1.5	2.0	26.9	23.3	6.2		0.27
InternVL2.5-8B [10]	50.0	55.0	33.6	41.1	59.1	8.4	14.8	8.7	12.9	1.5	47.8	10.6		0.2
InternVL2.5-26B [10]	62.6	55.4	33.0	50.2	61.8	30.5	32.0	13.3	17.3	32.8	52.6	25.2		0.49
Qwen2.5-VL-32B-Instruct [59]	48.9	36.8	32.3	31.1	30.1	25.6	6.9	8.0	10.4	12.9	35.8	12.8		0.36
InternVL2.5-38B [10]	64.4	54.3	36.8	45.6	63.0	47.8	37.9	7.3	21.3	46.8	52.8	32.0		0.61
LLaVA-OneVision-72B [24]	67.9	64.5	40.3	46.7	67.3	38.9	32.0	13.3	34.7	35.8	57.3	30.9		0.54
Qwen2.5-VL-72B-Instruct [59]	55.7	40.9	32.1	36.5	38.0	17.2	13.3	13.0	15.7	15.9	40.6	15.0		0.37
InternVL2.5-78B [10]	62.4	64.4	40.3	36.6	67.3	38.4	33.5	12.1	12.9	45.8	54.2	28.5		0.53

On the other hand, several models yield unexpectedly poor results. For instance, Cambrian-34B scores only 0.15—almost identical to the much smaller InternVL2.5-2B (0.14)—suggesting a significant deficiency in understanding spatial compositions and relationships. Similarly, although LLaVA-OneVision-72B achieves state-of-the-art performance in overall metrics, its multiple/single score of just 0.51 falls behind comparably sized models such as Qwen2.5-VL-72B (0.57) and InternVL2.5-78B (0.60), indicating a lingering tendency to overfit to single-choice formats.

These findings underscore the importance of addressing task format overfitting in future MLLMs training. They also reveal current limitations in compositional spatial intelligence, validating the value and potential of the proposed SpaCE-10 benchmark. By highlighting nuanced weaknesses in compositional spatial comprehension across diverse models, this benchmark serves as a crucial diagnostic tool for future spatial intelligence evaluation of MLLMs.

B.2 Pipeline Component Ablation

To systematically evaluate the contribution of each key component in the structured data generation pipeline to the accuracy of basic QA generation, we designed a stepwise ablation study. Specifically, we selected five QA task types (SA, OO, OS, EP, FP), and for each type, we randomly sampled 30 scenes, generating one question per scene. The accuracy of each generated question was manually verified by human experts.

The experimental results clearly demonstrate the cumulative gains of each module. Using the 2D Captioner alone as the baseline, the generated QA already showed relatively stable accuracy across

Table 7: **Ablation study of structural data generation pipeline.** We randomly sample 30 scenes for each type of QA and generate one QA for each scene. The results demonstrate the effectiveness of each component.

Component	SA	OO	OS	EP	FP	Average
2D Captioner	50.0	50.0	46.7	96.7	66.7	62.0
+ 3D Captioner	80.0	63.3	63.3	96.7	80.0	76.7 (+14.7)
+ Inspector	80.0	66.7	70.0	96.7	83.3	79.3 (+17.3)
+ Structural Data	86.7	76.7	76.7	96.7	83.3	84.0 (+22.0)

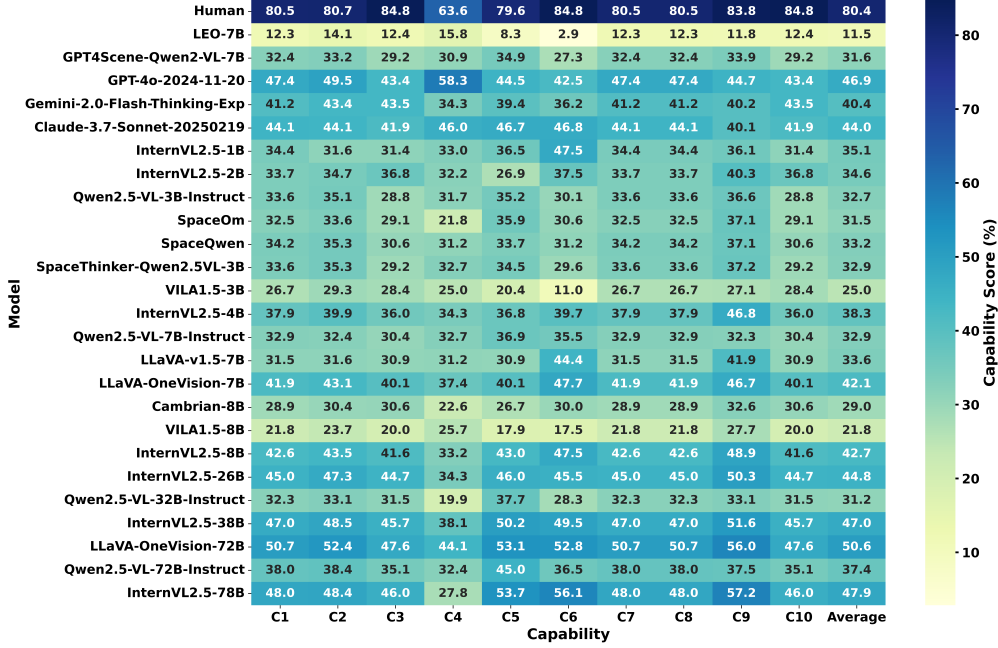
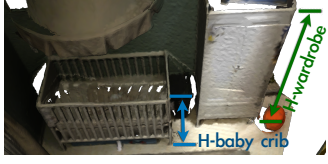


Figure 6: **Results of all tested MLLMs on 10 atomic capabilities of Space-10.** Each value reflects the model’s average accuracy (%) across all question types involving the respective spatial capability (C1–C10), as defined in the benchmark’s task-to-capability mapping.

most categories (an average of 62.0%), with particularly high accuracy in the EP task at 96.7%. This reflects the relatively low difficulty of generating questions for this category and that 2D visual information sufficiently supports it. With the addition of the 3D Captioner, the overall accuracy improved significantly (an average increase of 14.7%), indicating that 3D information effectively supplements the limitations of 2D vision and enhances the model’s understanding of spatial and object attributes. Further incorporating the Inspector component led to another increase in accuracy, reaching 79.3% (a 17.3% improvement over the baseline), showing that this module plays an important role in validating and refining the details of question generation. Finally, after adding structured data, the overall average accuracy reached 84.0%, a 22% improvement compared to the initial baseline, fully demonstrating the critical value of structured information in improving the quality of basic QA generation.

B.3 More Capability Assessment

In this section, we visualize all tested models’ capability performance in Fig. 6, which also presents the same tendency as Fig. 4 that the C5 counting ability is the most difficult for existing models.



Question: Which of the following statements accurately compares the relative sizes of a **white wooden baby crib** and a **wardrobe**?

A. The wardrobe is taller than the white wooden baby crib, but they are similar in width. ☒

B. The white wooden baby crib is both taller and wider than the wardrobe.

C. The wardrobe and the white wooden baby crib are the same height, but differ slightly in width.

D. The white wooden baby crib is significantly larger than the wardrobe in both height and width.

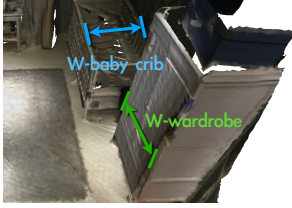


Figure 7: **Showcase of Basic SA QA.** ‘H’ and ‘W’ mean the height and width of objects, respectively. In this case, GPT-4o shows the precise understanding of both size and geometry.

C Case Study

C.1 Basic QA Quality

In this paper, we have developed a sophisticated pipeline for the automated generation of high-quality Basic QA (Basic Question Answering). In the previous section, we systematically verified the effectiveness of each component within the pipeline. This section presents two typical high-quality QA cases and delves into them with specific context-based analysis and discussion.

As shown in Fig. 7, the first case centers on the size estimation task (Basic SA). As depicted in the figure, through meticulously crafted prompts and high-quality snapshots, we steered GPT to accurately generate questions. When comparing the volume relationship between a white wooden baby crib and a wardrobe, GPT delivered an impressive performance. It not only correctly identified the height and width dimensions of each object but also precisely determined their relative differences across multiple perspectives. For instance, its response accurately pointed out that the wardrobe is taller than the crib but has a similar width, demonstrating a good grasp of the 3D geometric properties of objects.

The second case focuses on the spatial relationship understanding task (Basic OO), as shown in the Fig. 8, in the context of judging the spatial relationship between a yellow chair and an entrance. In this example, GPT not only accurately distinguished the relative direction of "left" but also correctly identified the spatial distance difference between "near" and "far". Although the question only involved one yellow chair, the distractors in the options were somewhat deceptive, which in turn enhanced the question’s ability to assess the model’s spatial understanding. This case also indirectly confirms the feasibility and rationality of using GPT for generating spatial intelligence QA questions. Through these two cases, we observed that powerful MLLMs, when only provided with high-quality 2D visual inputs, are already capable of understanding certain 3D spatial information, such as object size, volume relationships, and spatial orientation. This ability suggests a promising path for future exploration: unlike current 3D models that sacrifice conversational abilities to fit point cloud data, 2D MLLMs can still demonstrate strong spatial understanding potential even without explicitly incorporating 3D structural modeling.

C.2 Annotation Interface

To facilitate efficient annotation, we developed a custom annotation tool, with the interface shown in the Fig. 9. During the annotation process, human experts are restricted to viewing only 3D snapshots to judge the correctness of each QA pair—they are not allowed to view the 2D images. This design offers two main advantages: (1) It ensures a high annotation speed. By examining only a small number of 3D snapshots, annotators can quickly grasp the overall layout of the scene while significantly reducing their visual workload. (2) Since 2D images contain overly fine-grained

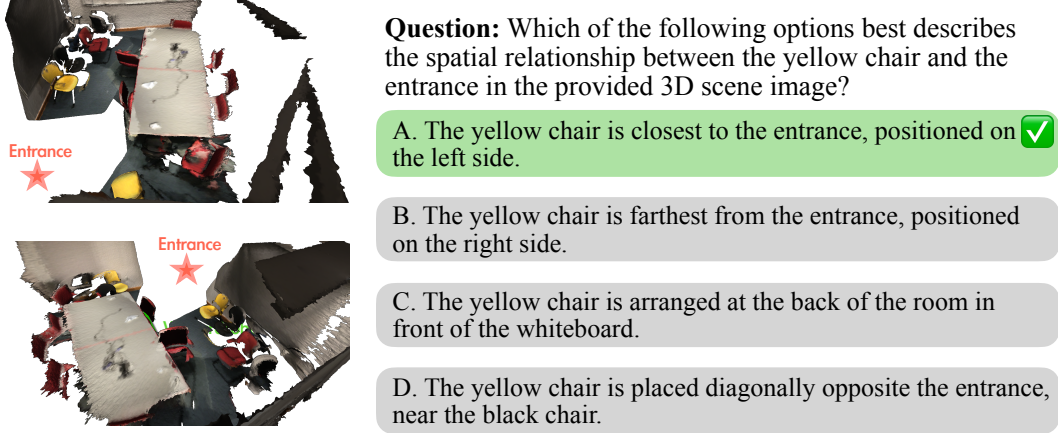


Figure 8: **Showcase of Basic OO QA.** This case reflects the capability in spatial relationships and QA design. Notably, all spatial relationship is based on the observation at the entrance.

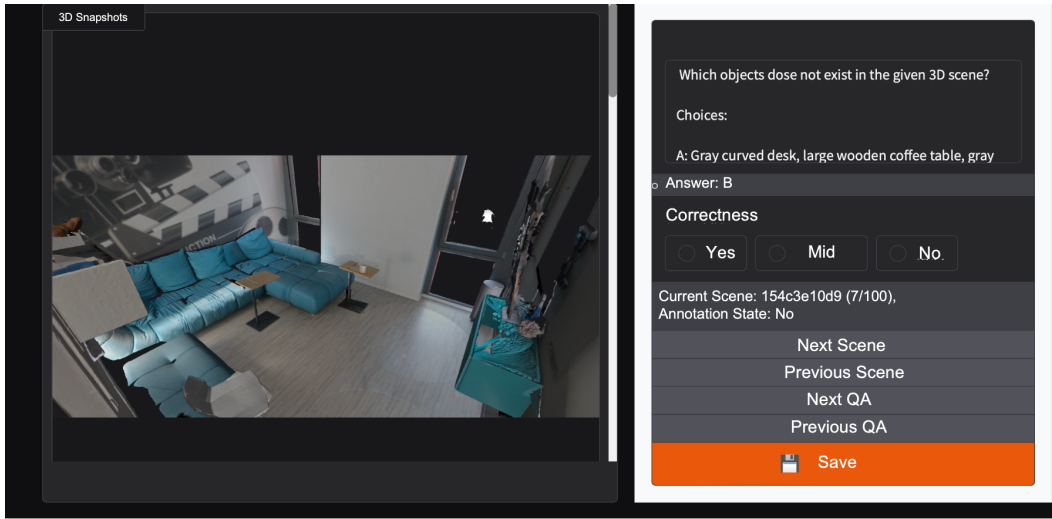


Figure 9: **Interface of annotation tools.**

details—many of which may not be present in the 3D scene—using only 3D information to filter out incorrect questions helps ensure that the resulting QA pairs are suitable for evaluation across both 2D and 3D models. Additionally, during evaluation, we tag erroneous questions to ensure none are overlooked. This end-to-end process not only prioritizes annotation efficiency but also reflects our rigorous commitment to data quality control.

References

- [1] The claude 3 model family: Opus, sonnet, haiku.
- [2] J. Achiam, S. Adler, S. Agarwal, L. Ahmad, I. Akkaya, F. L. Aleman, D. Almeida, J. Altenschmidt, S. Altman, S. Anadkat, et al. Gpt-4 technical report. *arXiv preprint arXiv:2303.08774*, 2023.
- [3] H. Agrawal, K. Desai, Y. Wang, X. Chen, R. Jain, M. Johnson, D. Batra, D. Parikh, S. Lee, and P. Anderson. Nocaps: Novel object captioning at scale. In *Proceedings of the IEEE/CVF international conference on computer vision*, pages 8948–8957, 2019.

- [4] D. Azuma, T. Miyanishi, S. Kurita, and M. Kawanabe. Scanqa: 3d question answering for spatial scene understanding. In *proceedings of the IEEE/CVF conference on computer vision and pattern recognition*, pages 19129–19139, 2022.
- [5] J. Bai, S. Bai, Y. Chu, Z. Cui, K. Dang, X. Deng, Y. Fan, W. Ge, Y. Han, F. Huang, et al. Qwen technical report. *arXiv preprint arXiv:2309.16609*, 2023.
- [6] S. Bai, K. Chen, X. Liu, J. Wang, W. Ge, S. Song, K. Dang, P. Wang, S. Wang, J. Tang, et al. Qwen2. 5-vl technical report. *arXiv preprint arXiv:2502.13923*, 2025.
- [7] G. Baruch, Z. Chen, A. Dehghan, T. Dimry, Y. Feigin, P. Fu, T. Gebauer, B. Joffe, D. Kurz, A. Schwartz, et al. Arkitscenes: A diverse real-world dataset for 3d indoor scene understanding using mobile rgb-d data. *arXiv preprint arXiv:2111.08897*, 2021.
- [8] D. Z. Chen, A. X. Chang, and M. Nießner. Scanrefer: 3d object localization in rgb-d scans using natural language. In *European conference on computer vision*, pages 202–221. Springer, 2020.
- [9] X. Chen, H. Fang, T.-Y. Lin, R. Vedantam, S. Gupta, P. Dollár, and C. L. Zitnick. Microsoft coco captions: Data collection and evaluation server. *arXiv preprint arXiv:1504.00325*, 2015.
- [10] Z. Chen, W. Wang, Y. Cao, Y. Liu, Z. Gao, E. Cui, J. Zhu, S. Ye, H. Tian, Z. Liu, et al. Expanding performance boundaries of open-source multimodal models with model, data, and test-time scaling. *arXiv preprint arXiv:2412.05271*, 2024.
- [11] Z. Chen, W. Wang, H. Tian, S. Ye, Z. Gao, E. Cui, W. Tong, K. Hu, J. Luo, Z. Ma, et al. How far are we to gpt-4v? closing the gap to commercial multimodal models with open-source suites. *Science China Information Sciences*, 67(12):220101, 2024.
- [12] Z. Chen, J. Wu, W. Wang, W. Su, G. Chen, S. Xing, M. Zhong, Q. Zhang, X. Zhu, L. Lu, et al. Internvl: Scaling up vision foundation models and aligning for generic visual-linguistic tasks. In *Proceedings of the IEEE/CVF conference on computer vision and pattern recognition*, pages 24185–24198, 2024.
- [13] A. Dai, A. X. Chang, M. Savva, M. Halber, T. Funkhouser, and M. Nießner. Scannet: Richly-annotated 3d reconstructions of indoor scenes. In *Proceedings of the IEEE conference on computer vision and pattern recognition*, pages 5828–5839, 2017.
- [14] W. Dai, J. Li, D. Li, A. M. H. Tiong, J. Zhao, W. Wang, B. A. Li, P. Fung, and S. C. Hoi. Instructblip: Towards general-purpose vision-language models with instruction tuning. *arxiv abs/2305.06500* (2023). URL: <https://api.semanticscholar.org/CorpusID/258615266>, 2023.
- [15] C. Fan, X. Jia, Y. Sun, Y. Wang, J. Wei, Z. Gong, X. Zhao, M. Tomizuka, X. Yang, J. Yan, et al. Interleave-vla: Enhancing robot manipulation with interleaved image-text instructions. *arXiv preprint arXiv:2505.02152*, 2025.
- [16] R. Fu, J. Liu, X. Chen, Y. Nie, and W. Xiong. Scene-llm: Extending language model for 3d visual understanding and reasoning. *arXiv preprint arXiv:2403.11401*, 2024.
- [17] Y. Goyal, T. Khot, D. Summers-Stay, D. Batra, and D. Parikh. Making the v in vqa matter: Elevating the role of image understanding in visual question answering. In *Proceedings of the IEEE conference on computer vision and pattern recognition*, pages 6904–6913, 2017.
- [18] Z. Guo, R. Zhang, X. Zhu, Y. Tang, X. Ma, J. Han, K. Chen, P. Gao, X. Li, H. Li, et al. Point-bind & point-llm: Aligning point cloud with multi-modality for 3d understanding, generation, and instruction following. *arXiv preprint arXiv:2309.00615*, 2023.
- [19] Y. Hong, H. Zhen, P. Chen, S. Zheng, Y. Du, Z. Chen, and C. Gan. 3d-llm: Injecting the 3d world into large language models. *Advances in Neural Information Processing Systems*, 36:20482–20494, 2023.
- [20] H. Huang, Y. Chen, Z. Wang, R. Huang, R. Xu, T. Wang, L. Liu, X. Cheng, Y. Zhao, J. Pang, et al. Chat-scene: Bridging 3d scene and large language models with object identifiers. In *The Thirty-eighth Annual Conference on Neural Information Processing Systems*, 2024.

- [21] J. Huang, S. Yong, X. Ma, X. Linghu, P. Li, Y. Wang, Q. Li, S.-C. Zhu, B. Jia, and S. Huang. An embodied generalist agent in 3d world. *arXiv preprint arXiv:2311.12871*, 2023.
- [22] D. A. Hudson and C. D. Manning. Gqa: A new dataset for real-world visual reasoning and compositional question answering. In *Proceedings of the IEEE/CVF conference on computer vision and pattern recognition*, pages 6700–6709, 2019.
- [23] M. Jia, Z. Qi, S. Zhang, W. Zhang, X. Yu, J. He, H. Wang, and L. Yi. Omnispatial: Towards comprehensive spatial reasoning benchmark for vision language models. *arXiv preprint arXiv:2506.03135*, 2025.
- [24] B. Li, Y. Zhang, D. Guo, R. Zhang, F. Li, H. Zhang, K. Zhang, P. Zhang, Y. Li, Z. Liu, et al. Llava-onevision: Easy visual task transfer. *arXiv preprint arXiv:2408.03326*, 2024.
- [25] J. Li, D. Li, S. Savarese, and S. Hoi. Blip-2: Bootstrapping language-image pre-training with frozen image encoders and large language models. In *International conference on machine learning*, pages 19730–19742. PMLR, 2023.
- [26] J. Li, D. Li, C. Xiong, and S. Hoi. Blip: Bootstrapping language-image pre-training for unified vision-language understanding and generation. In *International conference on machine learning*, pages 12888–12900. PMLR, 2022.
- [27] J. Li, G. Li, X. Zhang, Y. Dong, and Z. Jin. Evocodebench: An evolving code generation benchmark aligned with real-world code repositories. *arXiv preprint arXiv:2404.00599*, 2024.
- [28] M. Li, X. Chen, C. Zhang, S. Chen, H. Zhu, F. Yin, G. Yu, and T. Chen. M3dbench: Let’s instruct large models with multi-modal 3d prompts. *arXiv preprint arXiv:2312.10763*, 2023.
- [29] Y. Li, Z. Gong, H. Li, X. Huang, H. Kang, G. Bai, and X. Ma. Robotic visual instruction. *arXiv preprint arXiv:2505.00693*, 2025.
- [30] J. Lin, H. Yin, W. Ping, P. Molchanov, M. Shoybi, and S. Han. Vila: On pre-training for visual language models. In *Proceedings of the IEEE/CVF conference on computer vision and pattern recognition*, pages 26689–26699, 2024.
- [31] X. Linghu, J. Huang, X. Niu, X. S. Ma, B. Jia, and S. Huang. Multi-modal situated reasoning in 3d scenes. *Advances in Neural Information Processing Systems*, 37:140903–140936, 2024.
- [32] F. Liu, G. Emerson, and N. Collier. Visual spatial reasoning. *Transactions of the Association for Computational Linguistics*, 11:635–651, 2023.
- [33] H. Liu, C. Li, Y. Li, B. Li, Y. Zhang, S. Shen, and Y. J. Lee. Llvaneext: Improved reasoning, ocr, and world knowledge, 2024.
- [34] H. Liu, C. Li, Q. Wu, and Y. J. Lee. Visual instruction tuning. *Advances in neural information processing systems*, 36:34892–34916, 2023.
- [35] H. Liu, C. Li, Q. Wu, and Y. J. Lee. Visual instruction tuning. *Advances in neural information processing systems*, 36:34892–34916, 2023.
- [36] Y. Liu, Y. Cao, Z. Gao, W. Wang, Z. Chen, W. Wang, H. Tian, L. Lu, X. Zhu, T. Lu, et al. Mminstruct: A high-quality multi-modal instruction tuning dataset with extensive diversity. *Science China Information Sciences*, 67(12):1–16, 2024.
- [37] Y. Liu, H. Duan, Y. Zhang, B. Li, S. Zhang, W. Zhao, Y. Yuan, J. Wang, C. He, Z. Liu, et al. Mmbench: Is your multi-modal model an all-around player? In *European conference on computer vision*, pages 216–233. Springer, 2024.
- [38] Y. Liu, Z. Li, M. Huang, B. Yang, W. Yu, C. Li, X.-C. Yin, C.-L. Liu, L. Jin, and X. Bai. Ocrbench: on the hidden mystery of ocr in large multimodal models. *Science China Information Sciences*, 67(12):220102, 2024.
- [39] G. Luo, G. Yang, Z. Gong, G. Chen, H. Duan, E. Cui, R. Tong, Z. Hou, T. Zhang, Z. Chen, et al. Visual embodied brain: Let multimodal large language models see, think, and control in spaces. *arXiv preprint arXiv:2506.00123*, 2025.

- [40] G. Luo, X. Yang, W. Dou, Z. Wang, J. Liu, J. Dai, Y. Qiao, and X. Zhu. Mono-internvl: Pushing the boundaries of monolithic multimodal large language models with endogenous visual pre-training. *arXiv preprint arXiv:2410.08202*, 2024.
- [41] W. Ma, H. Chen, G. Zhang, C. M. de Melo, J. Chen, and A. Yuille. 3dsrbench: A comprehensive 3d spatial reasoning benchmark. *arXiv preprint arXiv:2412.07825*, 2024.
- [42] X. Ma, Y. Bhalgat, B. Smart, S. Chen, X. Li, J. Ding, J. Gu, D. Z. Chen, S. Peng, J.-W. Bian, et al. When llms step into the 3d world: A survey and meta-analysis of 3d tasks via multi-modal large language models. *arXiv preprint arXiv:2405.10255*, 2024.
- [43] X. Ma, S. Yong, Z. Zheng, Q. Li, Y. Liang, S.-C. Zhu, and S. Huang. Sqa3d: Situated question answering in 3d scenes. *arXiv preprint arXiv:2210.07474*, 2022.
- [44] K. Marino, M. Rastegari, A. Farhadi, and R. Mottaghi. Ok-vqa: A visual question answering benchmark requiring external knowledge. In *Proceedings of the IEEE/cvf conference on computer vision and pattern recognition*, pages 3195–3204, 2019.
- [45] Z. Qi, Z. Zhang, Y. Fang, J. Wang, and H. Zhao. Gpt4scene: Understand 3d scenes from videos with vision-language models. *arXiv preprint arXiv:2501.01428*, 2025.
- [46] A. Radford, J. W. Kim, C. Hallacy, A. Ramesh, G. Goh, S. Agarwal, G. Sastry, A. Askell, P. Mishkin, J. Clark, et al. Learning transferable visual models from natural language supervision. In *International conference on machine learning*, pages 8748–8763. PmLR, 2021.
- [47] S. K. Ramakrishnan, A. Gokaslan, E. Wijmans, O. Maksymets, A. Clegg, J. Turner, E. Under-sander, W. Galuba, A. Westbury, A. X. Chang, et al. Habitat-matterport 3d dataset (hm3d): 1000 large-scale 3d environments for embodied ai. *arXiv preprint arXiv:2109.08238*, 2021.
- [48] T. Saikh, T. Ghosal, A. Mittal, A. Ekbal, and P. Bhattacharyya. Scienceqa: A novel resource for question answering on scholarly articles. *International Journal on Digital Libraries*, 23(3):289–301, 2022.
- [49] E. Szymańska, M. Dusmanu, J.-W. Bui, M. Rad, and M. Pollefeys. Space3d-bench: Spatial 3d question answering benchmark. In *European Conference on Computer Vision*, pages 68–85. Springer, 2025.
- [50] G. Team, R. Anil, S. Borgeaud, J.-B. Alayrac, J. Yu, R. Soricut, J. Schalkwyk, A. M. Dai, A. Hauth, K. Millican, et al. Gemini: a family of highly capable multimodal models. *arXiv preprint arXiv:2312.11805*, 2023.
- [51] G. Team, P. Georgiev, V. I. Lei, R. Burnell, L. Bai, A. Gulati, G. Tanzer, D. Vincent, Z. Pan, S. Wang, et al. Gemini 1.5: Unlocking multimodal understanding across millions of tokens of context. *arXiv preprint arXiv:2403.05530*, 2024.
- [52] P. Tong, E. Brown, P. Wu, S. Woo, A. J. V. IYER, S. C. Akula, S. Yang, J. Yang, M. Middepogu, Z. Wang, et al. Cambrian-1: A fully open, vision-centric exploration of multimodal llms. *Advances in Neural Information Processing Systems*, 37:87310–87356, 2024.
- [53] S. Tong, Z. Liu, Y. Zhai, Y. Ma, Y. LeCun, and S. Xie. Eyes wide shut? exploring the visual shortcomings of multimodal llms. In *Proceedings of the IEEE/CVF Conference on Computer Vision and Pattern Recognition*, pages 9568–9578, 2024.
- [54] J. Wald, A. Avetisyan, N. Navab, F. Tombari, and M. Nießner. Rio: 3d object instance re-localization in changing indoor environments. In *Proceedings of the IEEE/CVF International Conference on Computer Vision*, pages 7658–7667, 2019.
- [55] Y. Xiao, E. Sun, T. Liu, and W. Wang. Logicvista: Multimodal llm logical reasoning benchmark in visual contexts. *arXiv preprint arXiv:2407.04973*, 2024.
- [56] R. Xu, X. Wang, T. Wang, Y. Chen, J. Pang, and D. Lin. Pointllm: Empowering large language models to understand point clouds. In *European Conference on Computer Vision*, pages 131–147. Springer, 2024.

- [57] W. Xu, J. Wang, W. Wang, Z. Chen, W. Zhou, A. Yang, L. Lu, H. Li, X. Wang, X. Zhu, et al. Visulogic: A benchmark for evaluating visual reasoning in multi-modal large language models. *arXiv preprint arXiv:2504.15279*, 2025.
- [58] X. Yan, Z. Yuan, Y. Du, Y. Liao, Y. Guo, S. Cui, and Z. Li. Comprehensive visual question answering on point clouds through compositional scene manipulation. *IEEE Transactions on Visualization and Computer Graphics*, 30(12):7473–7485, 2023.
- [59] A. Yang, B. Yang, B. Zhang, B. Hui, B. Zheng, B. Yu, C. Li, D. Liu, F. Huang, H. Wei, et al. Qwen2. 5 technical report. *arXiv preprint arXiv:2412.15115*, 2024.
- [60] A. Yang, B. Zhang, B. Hui, B. Gao, B. Yu, C. Li, D. Liu, J. Tu, J. Zhou, J. Lin, et al. Qwen2. 5-math technical report: Toward mathematical expert model via self-improvement. *arXiv preprint arXiv:2409.12122*, 2024.
- [61] J. Yang, S. Yang, A. W. Gupta, R. Han, L. Fei-Fei, and S. Xie. Thinking in space: How multimodal large language models see, remember, and recall spaces. *arXiv preprint arXiv:2412.14171*, 2024.
- [62] S. Yang, R. Xu, Y. Xie, S. Yang, M. Li, J. Lin, C. Zhu, X. Chen, H. Duan, X. Yue, et al. Mmsi-bench: A benchmark for multi-image spatial intelligence. *arXiv preprint arXiv:2505.23764*, 2025.
- [63] S. Ye, D. Chen, S. Han, and J. Liao. 3d question answering. *IEEE Transactions on Visualization and Computer Graphics*, 30(3):1772–1786, 2022.
- [64] C. Yeshwanth, Y.-C. Liu, M. Nießner, and A. Dai. Scannet++: A high-fidelity dataset of 3d indoor scenes. In *Proceedings of the IEEE/CVF International Conference on Computer Vision*, pages 12–22, 2023.
- [65] P. Young, A. Lai, M. Hodosh, and J. Hockenmaier. From image descriptions to visual denotations: New similarity metrics for semantic inference over event descriptions. *Transactions of the association for computational linguistics*, 2:67–78, 2014.
- [66] K. Zhang, B. Li, P. Zhang, F. Pu, J. A. Cahyono, K. Hu, S. Liu, Y. Zhang, J. Yang, C. Li, et al. Lmms-eval: Reality check on the evaluation of large multimodal models. *arXiv preprint arXiv:2407.12772*, 2024.
- [67] Y. Zhang, Z. Xu, Y. Shen, P. Kordjamshidi, and L. Huang. Spartun3d: Situated spatial understanding of 3d world in large language models. *arXiv preprint arXiv:2410.03878*, 2024.
- [68] L. Zhao, D. Cai, J. Zhang, L. Sheng, D. Xu, R. Zheng, Y. Zhao, L. Wang, and X. Fan. Toward explainable 3d grounded visual question answering: A new benchmark and strong baseline. *IEEE Transactions on Circuits and Systems for Video Technology*, 33(6):2935–2949, 2022.
- [69] C. Zhu, T. Wang, W. Zhang, J. Pang, and X. Liu. Llava-3d: A simple yet effective pathway to empowering lmms with 3d-awareness. *arXiv preprint arXiv:2409.18125*, 2024.
- [70] J. Zhu, W. Wang, Z. Chen, Z. Liu, S. Ye, L. Gu, Y. Duan, H. Tian, W. Su, J. Shao, et al. Internvl3: Exploring advanced training and test-time recipes for open-source multimodal models. *arXiv preprint arXiv:2504.10479*, 2025.
- [71] Y. Zhu, O. Groth, M. Bernstein, and L. Fei-Fei. Visual7w: Grounded question answering in images. In *Proceedings of the IEEE conference on computer vision and pattern recognition*, pages 4995–5004, 2016.